Available online at www.sciencedirect.com

ScienceDirect

journal homepage: http://www.elsevier.com/locate/acme

Original Research Article

Rapid heating induced vibration of circular cylindrical shells with magnetostrictive functionally graded material

C.C. Hong *

Department of Mechanical Engineering, Hsiuping University of Science and Technology, Taichung 412, Taiwan, ROC

ARTICLE INFO

Article history:
Received 3 May 2013
Accepted 29 October 2013
Available online 2 December 2013

Keywords:
Vibration
Rapid heating
FGM
Magnetostrictive
GDQ

ABSTRACT

The vibration and transient response of rapid heating on inner surface of the functionally graded material (FGM) circular cylindrical shells with outer magnetostrictive layer is investigated and computed by using the generalized differential quadrature (GDQ) method. The effects of heat flux value, power law index value, environmental temperature value and control gain value on Terfenol-D FGM circular cylindrical shell subjected to two edges clamped condition due to the not very high temperature fluid rapidly flow into the circular cylindrical shells from one side to the end of axial length direction are analyzed. The higher amplitudes of displacement and thermal stress can be obtained under the higher rapid heat flux value. With suitable product of coil constant and control gain value can reduce the amplitudes of displacement and thermal stress into a smaller value. The displacement of Terfenol-D FGM circular cylindrical shell versus the Terfenol-D thickness is stable for all power law index values. The Terfenol-D FGM circular cylindrical shell can stand against the higher temperature of environment with some values of power law index under rapid heating.

1. Introduction

The material properties of functionally graded material (FGM) usually considered and depended on the temperature of environment. Magnetostrictive material usually applied and controlled to the fields of sensors and actuators. In 2013, Kugler et al. [1] used the low-order shell element numerical method to investigate the beam-shell structures for FGM shells. In 2012, Mollarazi et al. [2] used an axis-symmetric weak form meshless method to analyze the free vibration of FGM cylinders. In 2012, Guz et al. [3] presented the dissipative heating induced vibration analysis for three-layer beam with piezoelectric layers. In 2012, Alibeigloo et al. [4] presented the numerical free vibration analysis for FGM cylindrical shell embedded thin piezoelectric layers. In 2011, Chen et al. [5] used the average stress method to investigate the thermal buckling for ceramic-FGM-metal plates. In 2011, Ootao et al. [6] analyzed and calculated the transient thermal stress for FGM strip composed of piezoelectric and magnetostrictive layers due to non-uniform surface heating. In 2007, Civalek [7] used the discrete singular convolution (DSC) approach method to solve linear vibration problem of isotropic conical shells. In 2007, Civalek [8] investigated the free vibration parameterization of rotating

* Tel.: +886 919037599; fax: +886 4 24961187.
E-mail address: cchong@mail.hust.edu.tw.

1644-9665/$ – see front matter
http://dx.doi.org/10.1016/j.acme.2013.10.012

laminated cylindrical shells by using the DSC method. In 2006, Civalek [9] presented the free vibration analysis of composite conical shells by using the DSC algorithm. In 2006, Bhangale et al. [10] used the first-order shear deformation theory (FSDT) of finite element method (FEM) to investigate the thermal buckling and free vibration behaviors for FGM conical shells in a high-temperature environment. In 2004, Manoach and Ribeiro [11] presented the nonlinear large amplitude vibrations of moderately thick beams under short heat flux and mechanical harmonic loading. In 2001, Cho and Kardomateas [12] presented a numerical dynamic thermal shock stresses result for a thick orthotropic cylindrical shell due to rapidly change of temperature. In 2000, Wojciechowski [13] presented the controlled purposes development of FGM in mechanical engineering usually composited of particular layers of piezoelectric, magnetostrictive, electrostrictive and shape memory alloys. In 1994, Chang and Shyong [14] used the FEM to compute and find the transient response results for laminated circular cylindrical shell under thermal impact. In 1993, Huang and Tauchert [15] used the FEM to calculate the large-amplitude vibration result for graphite-reinforced aluminum cylindrical panels during a sudden rise in surface temperature. In 1980, Manolis and Beskos [16] used the general numerical method to investigate the vibrations response of beam structures under rapidly thermal loads. In 1982, Shirakawa [17] presented the numerical dynamic responses of displacements and stresses for an orthotropic cylindrical shell due to rapid heating.

In the literature same title problem can be solved via different approach. The main superiority of presented method generalized differential quadrature (GDQ) used to solve the title problem, get acceptable results with less grid and computational time in the not higher modes. Namely, by using the axis-symmetric elements FEM is more effectively used for title problem in the higher modes. The author has some computational experiences and solutions in the piezoelectric shells and magnetostrictive plates by using the GDQ method. In 2013, Hong [18] investigated transient response of stress and displacement for magnetostrictive FGM square plates under rapid heating. In 2012, Hong [19] investigated the stress and displacement of magnetostrictive FGM plates in rapid heating by considering the effects: thickness of Terfenol-D, control gains, rapid heating flux and power law index of SUS304-Si_3N_4 materials. In 2010, Hong [20] computed and presented the solutions of thermal transient response of magnetostrictive plates. In 2010, Hong [21] investigated the behaviors of displacement and stresses of piezoelectric shells under the electromechanical loads. In 2009, Hong [22] investigated and obtained the thermal vibration of axial, circumferential and normal displacements of laminated shells under rapid heating. Usually the FGM shell work is motivated in the higher temperature environment as shielding and might be induced vibration due to rapid heating. A reducing vibration subject of practical solution might be the use of magnetostrictive material layer onto the surface of FGM shells. It is interesting to study the thermal vibration and transient responses of displacement and stress, with and without the effect of velocity feedback, respectively in the magnetostrictive FGM shell under rapid heating due to the not very high temperature fluid rapidly flow into the circular cylindrical shells from one side to the end of axial length direction by using the GDQ method.

2. Formulation

2.1. FGM

The Young's modulus is usually in great value of GPa (10^9 N/m^2) unit, so it is the main and dominant properties when compared with others. For the calculation simplification in stiffness integrations of FGM circular cylindrical shell, it is reasonable to assume only the Young's modulus is in the power law function of two-material FGM shell, the others properties are all in the average forms. The Young's modulus for the power law function of two-material FGM circular cylindrical shell as shown in Fig. 1 is expressed in the following equation in 2006 by Chi and Chung [23]

$$E_{fgm} = (E_2 - E_1)\left(\frac{z + h/2}{h}\right)^{R_n} + E_1, \tag{1a}$$

$$\kappa_{fgm} = \frac{\kappa_2 + \kappa_1}{2}, \tag{1b}$$

$$\alpha_{fgm} = \frac{\alpha_2 + \alpha_1}{2}, \tag{1c}$$

$$\rho_{fgm} = \frac{\rho_2 + \rho_1}{2}, \tag{1d}$$

$$\nu_{fgm} = \frac{\nu_2 + \nu_1}{2}. \tag{1e}$$

where z is the thickness coordinate, h is the thickness of FGM shells. R_n is the power law index. E_{fgm}, E_1 and E_2 are the Young's modulus, κ_{fgm}, κ_1 and κ_2 are the thermal conductivities, α_{fgm}, α_1 and α_2 are the thermal expansion coefficients, ρ_{fgm}, ρ_1 and ρ_2 are the densities, ν_{fgm}, ν_1 and ν_2 are the Poisson's ratios, respectively to the FGM shells, the constituent FGM material 1 and FGM material 2. The term of properties E_1, E_2, κ_1, κ_2, α_2, α_1, ρ_1, ρ_2, ν_1 and ν_2 can be expressed corresponding to the individual properties term P_i in constituent material equation $P_i = P_0(P_{-1}T^{-1} + 1 + P_1T + P_2T^2 + P_3T^3)$ in which P_0, P_{-1}, P_1, P_2 and P_3 are the temperature coefficients, T is the temperature of environment.

2.2. Stress–strain relations with magnetostrictive effect

A thin multilayered of magnetostrictive FGM circular cylindrical shells subjected to rapid heating on inner surface is considered as shown in Fig. 1, the thermo elastic stress–strain relationship of the kth layer (denoted in the subscript (k)) including thermal strain and magnetostrictive coupling effect are expressed in the following equations in 2006 by Lee et al. [24].

$$\begin{Bmatrix} \sigma_x \\ \sigma_\theta \\ \sigma_{x\theta} \end{Bmatrix}_{(k)} = \begin{bmatrix} \overline{Q}_{11} & \overline{Q}_{12} & \overline{Q}_{16} \\ \overline{Q}_{12} & \overline{Q}_{22} & \overline{Q}_{26} \\ \overline{Q}_{16} & \overline{Q}_{26} & \overline{Q}_{66} \end{bmatrix}_{(k)} \begin{Bmatrix} \varepsilon_x - \alpha_x \Delta T \\ \varepsilon_\theta - \alpha_\theta \Delta T \\ \varepsilon_{x\theta} - \alpha_{x\theta} \Delta T \end{Bmatrix}_{(k)} - \begin{bmatrix} 0 & 0 & \overline{e}_{31} \\ 0 & 0 & \overline{e}_{32} \\ 0 & 0 & \overline{e}_{36} \end{bmatrix}_{(k)} \begin{Bmatrix} 0 \\ 0 \\ \tilde{H}_z \end{Bmatrix}_{(k)}. \tag{2}$$

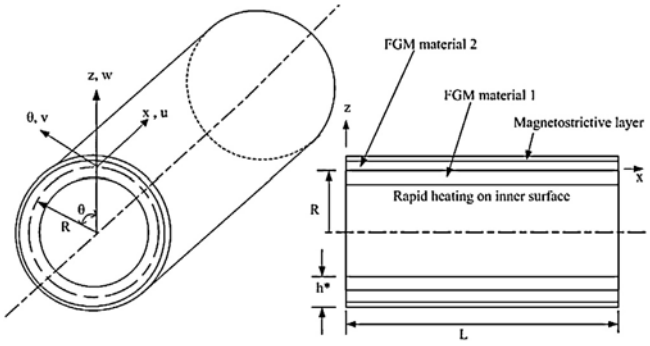

Fig. 1 – Geometry of magnetostrictive two-material FGM shells under rapid heating.

where σ_x, σ_θ and $\sigma_{x\theta}$ are thermal stresses. α_x and α_θ are the coefficients of thermal expansion, $\alpha_{x\theta}$ is the coefficient of thermal shear in the kth layer, they are corresponding to α_1 in the FGM material 1 layer, corresponding to α_2 in the FGM material 2 layer and use the magnetostrictive coefficients in the magnetostrictive layer. ΔT is the temperature difference between the shell and curing area. $\overline{Q}_{ij}$ is the stiffness. ε_x, ε_θ and $\varepsilon_{x\theta}$ are strains. $\bar{e}_{ij}$ is the transformed magnetostrictive coupling modulus. $\tilde{H}_z$ is the magnetic field intensity can be expressed in the following velocity feedback control equations in 2004 by Lee et al. [25].

$$\tilde{H}_z(x,y,t) = k_c c(t)\frac{\partial w}{\partial t}. \tag{3}$$

in which k_c is the coil constant, $c(t)$ is the control gain, w is displacement component in the z direction, t is the time.

The strains in terms of displacement components without the effects of shear deformation are expressed in the following equations.

$$\varepsilon_x = \frac{\partial u}{\partial x} - \frac{\partial^2 w}{\partial x^2}z, \tag{4a}$$

$$\varepsilon_\theta = \frac{1}{R}\left(\frac{\partial}{\partial\theta} + w\right) - \frac{1}{R^2}\left(\frac{\partial^2 w}{\partial\theta^2} - \frac{\partial v}{\partial\theta}\right)z, \tag{4b}$$

$$\varepsilon_{x\theta} = \frac{\partial v}{\partial x} + \frac{1}{R}\frac{\partial u}{\partial\theta} - 2\frac{1}{R}\left(\frac{\partial^2 w}{\partial x\partial\theta} - \frac{\partial v}{\partial x}\right)z. \tag{4c}$$

in which u and v are displacement components in the x and θ direction, respectively, R is the mean radius. x, θ and z are the cylindrical coordinates system fixed on the middle surface of the cylinder.

The simple forms of $\overline{Q}_{ij}$ are used for the FGM and without considering the angle effects of FGM fiber directions, are expressed in the following equations in 2007 by Shen [26].

$$\overline{Q}_{11} = \overline{Q}_{22} = \frac{E_{fgm}}{1-\nu_{fgm}^2}, \tag{5a}$$

$$\overline{Q}_{12} = \frac{\nu_{fgm}E_{fgm}}{1-\nu_{fgm}^2}, \tag{5b}$$

$$\overline{Q}_{66} = \frac{E_{fgm}}{2(1+\nu_{fgm})}, \tag{5c}$$

$$\overline{Q}_{16} = \overline{Q}_{26} = 0. \tag{5d}$$

The simple forms of $\overline{Q}_{ij}$ with Poisson's ratios $\upsilon = 0$ are used for the layer of magnetostrictive material, are expressed in the following equations.

$$\overline{Q}_{11} = \overline{Q}_{22} = E_{11}, \tag{5e}$$

$$\overline{Q}_{66} = \frac{E_{11}}{2}, \tag{5f}$$

$$\overline{Q}_{12} = \overline{Q}_{16} = \overline{Q}_{26} = 0. \tag{5g}$$

in which E_{11} is the Young's modulus for the magnetostrictive material.

2.3. *GDQ method*

The GDQ method is used to approximate the derivatives of functions by Shu and Richards and reviewed as follows: the derivative of a smooth function at a discrete point can be discretized by using a weighting linear sum of the function values at all the discrete point in1997 by Shu and Du [27].

2.4. *Dynamic equilibrium differential equations*

For thin multilayered magnetostrictive FGM circular cylindrical shell under the pulsating axial load, the thermally dynamic equilibrium differential equations without angular rotating axial speeds and without considering the shear deformation effects, in terms of displacement components included the effect of mth layer magnetostrictive loads are expressed in the following equations in 1998 by Hua and Lam [28].

$$\begin{bmatrix} L_{11} & L_{12} & L_{13} \\ L_{21} & L_{22} & L_{23} \\ L_{31} & L_{32} & L_{33} \end{bmatrix}\begin{Bmatrix} u \\ v \\ w \end{Bmatrix} = \begin{Bmatrix} b_1 \\ b_2 \\ b_3 \end{Bmatrix}. \tag{6}$$

in which L_{ij} is the partial derivative terms with coefficients A_{ij}, B_{ij} and D_{ij}, i = 1, 2, 3, j = 1, 2, 3.

$$b_1 = \frac{\partial\overline{N}_x}{\partial x} + \frac{1}{R}\frac{\partial\overline{N}_{x\theta}}{\partial\theta} + \frac{\partial\tilde{N}_x}{\partial x} + \frac{1}{R}\frac{\partial\tilde{N}_{x\theta}}{\partial\theta},$$

$$b_2 = \frac{\partial\overline{N}_{x\theta}}{\partial x} + \frac{1}{R}\frac{\partial\overline{N}_\theta}{\partial\theta} + \frac{1}{R}\frac{\partial\overline{M}_{x\theta}}{\partial x} + \frac{1}{R^2}\frac{\partial\overline{M}_\theta}{\partial\theta} + \frac{\partial\tilde{N}_{x\theta}}{\partial x} + \frac{1}{R}\frac{\partial\tilde{N}_\theta}{\partial\theta} + \frac{1}{R}\frac{\partial\tilde{M}_{x\theta}}{\partial x} + \frac{1}{R^2}\frac{\partial\tilde{M}_\theta}{\partial\theta},$$

$$b_3 = \frac{\partial^2\overline{M}_x}{\partial x^2} + \frac{2}{R}\frac{\partial^2\overline{M}_{x\theta}}{\partial x\partial\theta} + \frac{1}{R^2}\frac{\partial^2\overline{M}_\theta}{\partial\theta^2} - \frac{\overline{N}_\theta}{R} + \frac{\partial^2\tilde{M}_x}{\partial x^2} + \frac{2}{R}\frac{\partial^2\tilde{M}_{x\theta}}{\partial x\partial\theta} + \frac{1}{R^2}\frac{\partial^2\tilde{M}_\theta}{\partial\theta^2} - \frac{\tilde{N}_\theta}{R},$$

$$(A_{ij}, B_{ij}, D_{ij}) = \int_{-h^*/2}^{h^*/2}\overline{Q}_{ij}(1, z, z^2)dz,$$

$$(\overline{N}_x, \overline{M}_x) = \int_{-h^*/2}^{h^*/2}(\overline{Q}_{11}\alpha_x + \overline{Q}_{12}\alpha_\theta + \overline{Q}_{16}\alpha_{x\theta})\Delta T(1, z)dz,$$

$$(\overline{N}_\theta, \overline{M}_\theta) = \int_{-h^*/2}^{h^*/2} (\overline{Q}_{12}\alpha_x + \overline{Q}_{22}\alpha_\theta + \overline{Q}_{26}\alpha_{x\theta})\Delta T(1,z)dz,$$

$$(\overline{N}_{x\theta}, \overline{M}_{x\theta}) = \int_{-h^*/2}^{h^*/2} (\overline{Q}_{16}\alpha_x + \overline{Q}_{26}\alpha_\theta + \overline{Q}_{66}\alpha_{x\theta})\Delta T(1,z)dz,$$

$$\begin{Bmatrix} \tilde{N}_x \\ \tilde{N}_\theta \\ \tilde{N}_{x\theta} \end{Bmatrix} = \sum_{k=1}^{N_m} \int_{z_k}^{z_{k+1}} \begin{Bmatrix} \bar{e}_{31} \\ \bar{e}_{32} \\ \bar{e}_{36} \end{Bmatrix}_{(m)} \tilde{H}_z dz,$$

$$\begin{Bmatrix} \tilde{M}_x \\ \tilde{M}_\theta \\ \tilde{M}_{x\theta} \end{Bmatrix} = \sum_{k=1}^{N_m} \int_{z_k}^{z_{k+1}} \begin{Bmatrix} \bar{e}_{31} \\ \bar{e}_{32} \\ \bar{e}_{36} \end{Bmatrix}_{(m)} \tilde{H}_z z^2 dz.$$

where N_m is the number of magnetostrictive layer, the subscript m denotes the magnetostrictive layer. h^* is the total thickness of magnetostrictive layer and FGM shell. $\overline{N}_x$, $\overline{N}_\theta$ and $\overline{N}_{x\theta}$ are expansion force resultants due to temperature field difference. $\overline{M}_x$, $\overline{M}_\theta$ and $\overline{M}_{x\theta}$ are expansion moment resultants due to temperature field difference. $\tilde{N}_x$, $\tilde{N}_\theta$ and $\tilde{N}_{x\theta}$ are expansion force resultants due to magnetostrictive loads. $\tilde{M}_x$, $\tilde{M}_\theta$ and $\tilde{M}_{x\theta}$ are expansion moment resultants due to magnetostrictive loads.

2.5. *Dynamic discretized equations*

The thermal vibration case is considered for the condition of expansion strain distribution which is independent of x, θ and an even function of z, with $\overline{N}_x = -N_a x$, N_a is the pulsating axial load, $\Delta T = (A_{11}/R^2)T_0 x$ as the thermally expansion load which is dependent of x and T_0, where T_0 is thermal temperature due to rapid uniform heating on inner surface of FGM circular cylindrical shells, on the outer surface and edges of the magnetostrictive FGM circular cylindrical shells are assumed in thermally insulated, thus the conventional equation of temperature field T_0 is function of z and t, can be used directly as follows in1987 by Hetnarski [29].

$$T_0 = \frac{h^* q_0}{\kappa_{fgm}} \times \left[\frac{\beta t}{\pi^2} + \frac{1}{2}\left(-\frac{z}{h^*} + \frac{1}{2}\right)^2 - \frac{1}{6} - \frac{2}{\pi^2}\sum_{j=1}^{\infty} \frac{(-1)^j}{j^2} e^{-j^2\beta t} \cos j\pi\left(-\frac{z}{h^*} + \frac{1}{2}\right)\right]. \tag{7a}$$

in which $\beta = \pi^2\kappa_{fgm}/h^{*2}$, q_0 is the applied heat flux.

This conventional equation of temperature field T_0 is developed from the heat transfer equation as follows.

$$\frac{\partial T_0}{\partial t} = \kappa_{fgm}\frac{\partial^2 T_0}{\partial z^2} \tag{7b}$$

and the boundary conductions are specified at inner and outer surface of the circular cylindrical shells as follows.

$$\kappa_{fgm}\frac{\partial T_0(-h^*/2, t)}{\partial z} = q_0 \tag{7c}$$

$$\frac{\partial T_0(h^*/2, t)}{\partial z} = 0 \tag{7d}$$

and with the initial condition: $T_0(z, 0) = 0$

The physical investigation for the assumed boundary condition is to calculate the some ΔT effects of rapid heating at the inner surface of FGM shells due to the not very high temperature fluid rapidly flow into the circular cylindrical shells from $x = 0$ to $x = L$. By the way, the flow stress due to plastic strain in very high temperature would happen.

For the A_{11} calculation in stiffness integrations of magnetostrictive FGM shells, the following equation can be obtained.

$$A_{11} = \frac{h}{1 - ((\nu_1 + \nu_2)/2)^2}\left(\frac{R_n E_1 + E_2}{R_n + 1}\right) + E_{11}h_3. \tag{8}$$

in which h_3 is the thickness of magnetostrictive layer, υ_1 and υ_2 are the Poisson's ratios of individual constituent FGMs.

The following displacement components are investigated in triangular functions.

$$u = U(x)\cos(n\theta + \omega t), \tag{9a}$$

$$v = V(x)\sin(n\theta + \omega t), \tag{9b}$$

$$w = W(x)\cos(n\theta + \omega t). \tag{9c}$$

where $U(x)$, $V(x)$ and $W(x)$ are the amplitude functions of vibration mode of the displacement components in longitudinal direction. ω (rad/s) is the natural circular frequency and mode shape n is an integer for the circumferential wave number of the multilayered shells.

The one-dimensional GDQ method is applied to discretize the equilibrium differential equations and introduce the following non-dimensional parameters.

$$X = \frac{x}{L}, \tag{10a}$$

$$U = \frac{U(x)}{L}, \tag{10b}$$

$$V = \frac{V(x)}{R}, \tag{10c}$$

$$W = \frac{W(x)}{h^*}, \tag{10d}$$

$$Z = \frac{z}{h^*}. \tag{10e}$$

where L is the length of shell, h^* is the total thickness of magnetostrictive FGM shells.

Considering for two edges are clamped, symmetric ($B_{ij} = 0$), orthotropic ($A_{16} = A_{26} = 0$, $D_{16} = D_{26} = 0$, $\sigma_{x\theta} = 0$) of laminated shell under temperature loading, thus the dynamic discretized equilibrium equations and the following frequency parameter can be obtained.

$$f^* = \omega R\sqrt{\rho_t/A_{11}} \tag{11a}$$

$$\rho_t = \int_{-h^*/2}^{h^*/2} \rho dz \tag{11b}$$

in which ρ is the density of magnetostrictive FGM shell.

3. Computational results

The standard finite element method common usually used to solve, apply a problem and more commercial program had been derived for the source. It is interesting to writing the GDQ computing program by oneself and solving the rapid heating problem of Terfenol-D FGM circular cylindrical shells. Type of boundary conditions and mode numbers usually affect the best results for the same grid numbers. The following equation of coordinate is used for the grid point in the GDQ computation.

$$x_i = 0.5\left[1 - \cos\left(\frac{i-1}{N-1}\pi\right)\right]L, \quad i = 1, 2, \ldots, N \tag{12}$$

where N is the total discrete grid points number used in the x direction.

The total three-layer magnetostrictive FGM circular cylindrical shell as shown in Fig. 1 is considered with the outer surface magnetostrictive layer is Terfenol-D, the inner layers of the FGM material 1 is Si_3N_4, the FGM material 2 is SUS304. The thickness of FGM material 1 and FGM material 2 is denoted as h_1 and h_2, respectively. Considering h_1 is equal to h_2 in the GDQ computation. Firstly, the dynamic convergence of the frequency parameter f^* and center displacement $W|_{X=0.5}$ are investigated and compared with $R/h = 500$, $L/R = 10$, circumferential wave number $n = 4$, rapid heat flux value $q_0 = 2110$ J/(sm^2), $\theta = 1$ radian, time $t = 1$ s, Terfenol-D thickness ratio $h_3/h^* = 0.1$, environmental temperature value $T = 500$ K, $R_n = 1$ and without velocity feedback $k_c c(t) = 0$ under clamped–clamped boundary condition. Table 1 shows the f^* value and $W|_{X=0.5}$ value with respect to grid point N value for rapid heating on inner surface of the Terfenol-D FGM shells. More accurate results and less grid points are more suitable for all kind boundary and higher modes of vibration are investigated by using the harmonic differential quadrature (HDQ) method in 2004 by Civalek [30]. For the simplification, we only consider the clamped–clamped boundary condition and modes of vibration $n = 1$–9. The central processing unit Intel Pentium M processor 1.73 GHz of notebook is used in the calculation to give a preliminary view on the accuracy of the solution and the computation time. The real computation time took 1 s in each number of grid point convergence calculation. The accuracy of f^* values is 5.4×10^{-5} for $N = 49$ grid point, it is acceptable for the preliminary study. The computational results of grid point $N = 49$ are found in the acceptable convergence and can be used further for the rapid heating responses of displacement and stress.

The dominant displacement and stress values under rapid heating are also investigated and compared. Fig. 2a shows the

Table 1 – Dynamic convergence of GDQ results in rapid heating.

N	f^*	Accuracy of f^*	$W\|_{X=0.5}$
23	0.0107143		−0.881667
29	0.0125000	1.4×10^{-1}	−1.88422
33	0.0128564	2.7×10^{-2}	−2.52597
49	0.0128571	5.4×10^{-5}	−2.53058

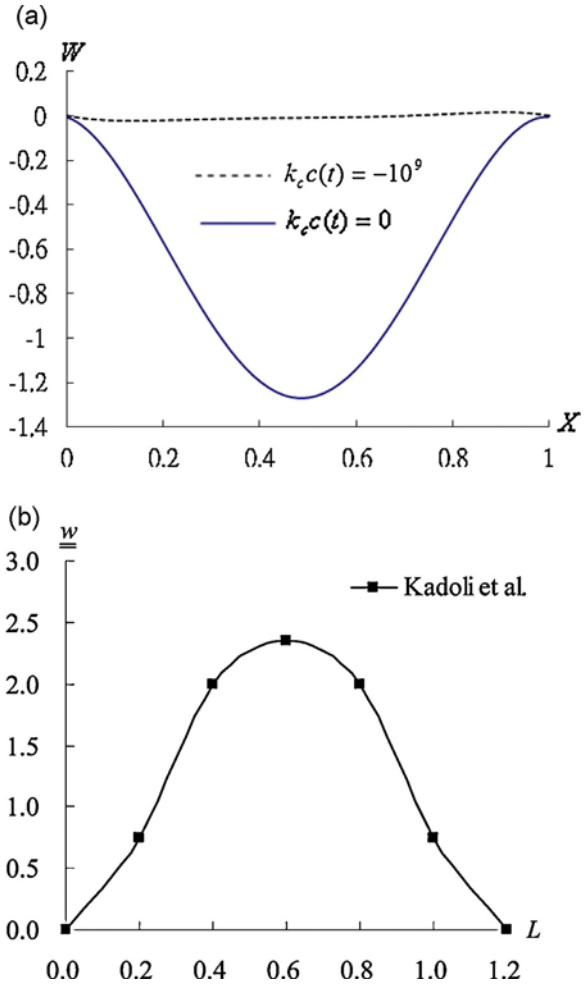

Fig. 2 – Comparison of the displacement (deflection) vs. the length. (a) W vs. X of rapid heating Terfenol-D FGM shells. (b) $\underline{w}$ vs. L of FGM beams.

dominant normal displacement W along X of rapid heating on inner surface of the Terfenol-D FGM shells under the effects of control gain values $k_c c(t) = 0$ and -10^9 cases, $h_3/h^* = 0.1$, rapid heat flux value $q_0 = 1055$ J/(sm^2), $T = 500$ K, $R_n = 1$, $\theta = 1$ radian, time $t = 1$ s. The great amplitude of displacement W value is -1.27 occurred at $X = 0.5$ when without velocity feedback ($k_c c(t) = 0$). We find that with velocity feedback and with suitable control gain value $k_c c(t) = -10^9$ can reduce the amplitude of displacement to a smaller value ($W = -8.94E{-}03$ at $X = 0.5$). The values W versus X are also compared with non-dimensional deflection $\underline{w}$ versus L in 2008 by Kadoli et al. [31], where $\underline{w} = 100WbE_{mental}h^3/(FL^4)$, E_{mental} is the Young's modulus of SUS304 and F is the applied mechanical load. The referred data as shown in Fig. 2b is re-plotted for the SUS304-Si_3N_4 FGM beam included higher order shear deformation with clamped-clamped ends. Fig. 2 shows the good similar tendency of W and $\underline{w}$ versus L, but the different scalar values occur between two plots are acceptable for the available referred data in different parameter definitions.

Fig. 3a shows the dominant thermal normal stress $\overline{\sigma}_x = \sigma_x/E_2$ on $Z = 0.4$ along X of rapid heating on inner surface of the

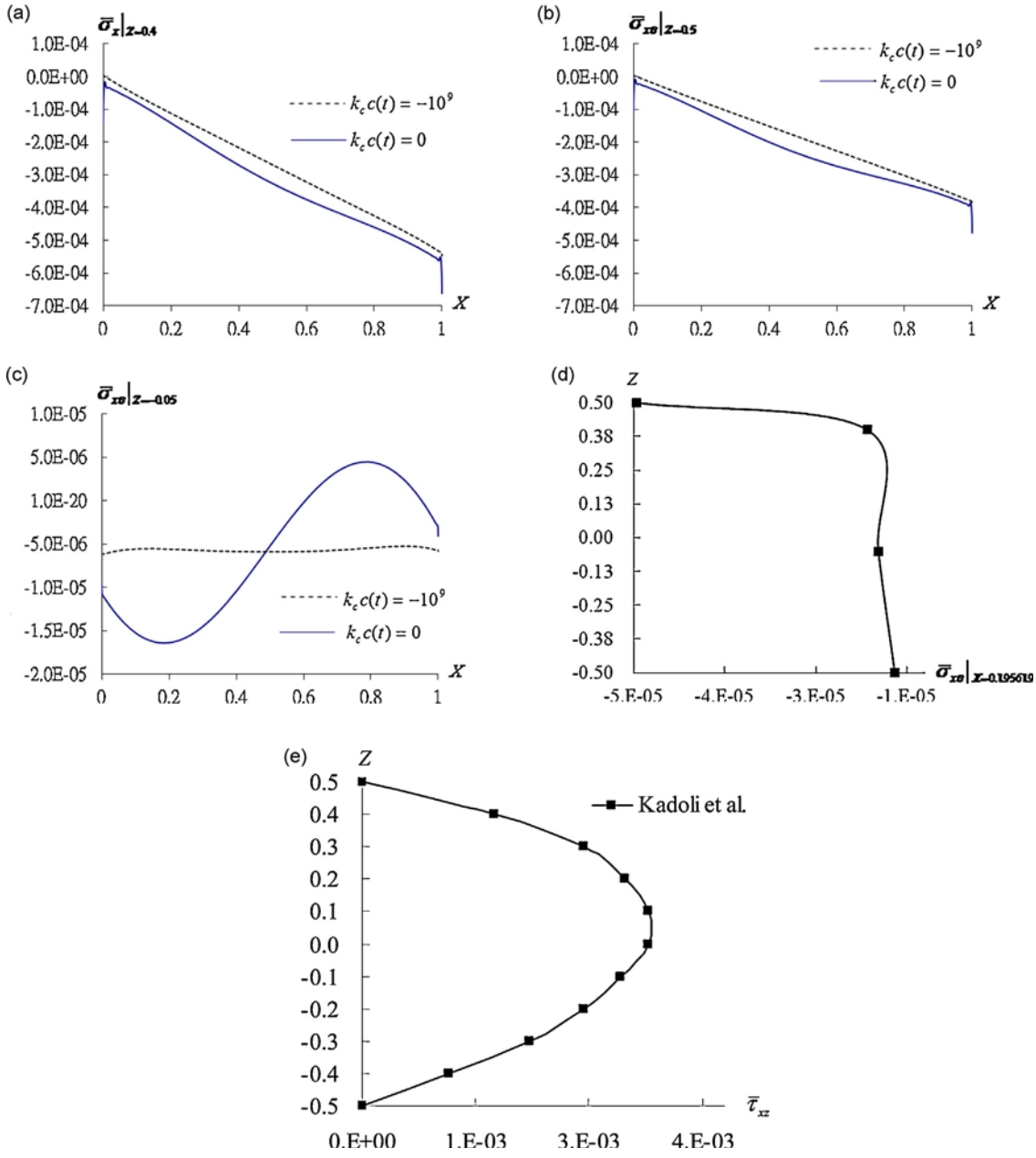

Fig. 3 – $\bar{\sigma}_x|_{Z=0.4}$ vs. X, $\bar{\sigma}_{x\theta}|_{Z=0.5}$ vs. X, $\bar{\sigma}_{x\theta}|_{Z=-0.05}$ vs. X and $\bar{\sigma}_{x\theta}|_{X=0.195619}$ vs. Z. (a) $\bar{\sigma}_x|_{Z=0.4}$ vs. X under control gain values $k_c c(t)$. (b) $\bar{\sigma}_{x\theta}|_{Z=0.5}$ vs. X under control gain values $k_c c(t)$. (c) $\bar{\sigma}_{x\theta}|_{Z=-0.05}$ vs. X under control gain values $k_c c(t)$. (d) $\bar{\sigma}_{x\theta}|_{X=0.195619}$ vs. Z of Terfenol-D FGM shells under rapid heating. (e) Comparison $\bar{\tau}_{xz}$ vs. Z of FGM beams under no thermal load.

Terfenol-D FGM shells under the effects of control gain values $k_c c(t) = 0$ and -10^9 cases, $h_3/h^* = 0.1$, rapid heat flux value $q_0 = 1055$ J/(sm^2), $T = 500$ K, $R_n = 1$, $\theta = 1$ radian, time $t = 1$ s. When without velocity feedback $k_c c(t) = 0 = 0$, the amplitude of thermal normal stress $\bar{\sigma}_x|_{Z=0.4}$ is large, linearly increasing with X, and have a striking value $\bar{\sigma}_x = -6.61\text{E}-04$ on the end $X = 1$ due to the thermal load (ΔT) effect. When with velocity feedback and with suitable control gain value $k_c c(t) = -10^9$, the amplitude of thermal normal stress $\bar{\sigma}_x|_{Z=0.4}$ can be reduced to a little smaller value. Fig. 3b shows the dominant thermal shear stress $\bar{\sigma}_{x\theta} = \sigma_{x\theta}/E_2$ on $Z = 0.5$ along X of rapid heating on inner surface of the Terfenol-D FGM shells under the effects of $k_c c(t) = 0$ and -10^9 cases. When with velocity feedback and with suitable control gain value $k_c c(t) = -10^9$, the amplitude of thermal shear stress $\bar{\sigma}_{x\theta}|_{Z=0.5}$ can be reduced to a little smaller value. Fig. 3c shows the dominant thermal shear stress $\bar{\sigma}_{x\theta}$ on $Z = -0.05$ along X of rapid heating on inner surface of the Terfenol-D FGM shells under the effects of $k_c c(t) = 0$ and -10^9 cases. When without velocity feedback $k_c c(t) = 0$, the amplitude of thermal shear stress $\bar{\sigma}_{x\theta}|_{Z=-0.05}$ is large and oscillate in harmonic with X. There are great shear stress value $\bar{\sigma}_{x\theta} = -1.64\text{E}-05$ on the surface $X = 0.195619$ of Terfenol-D FGM shells due to the rapid heating thermal load (ΔT) effect. The values $\bar{\sigma}_{x\theta}$ versus Z on the surface $X = 0.195619$ as shown in Fig. 3d are also compared with the non-dimensional transverse shear stress $\bar{\tau}_{xz}$ versus Z of some available referred data

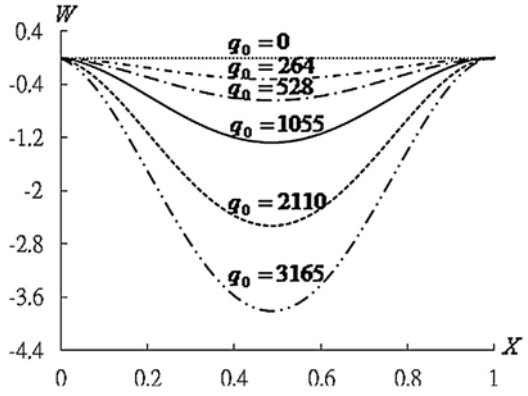

Fig. 4 – W vs. X under rapid heat flux q_0.

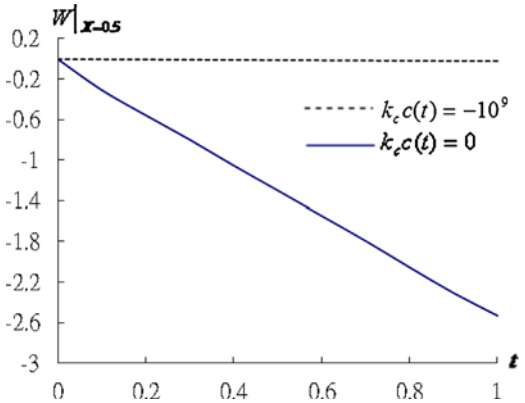

Fig. 6 – $W|_{X=0.5}$ vs. t (s) of rapid heating Terfenol-D FGM shells.

in 2008 by Kadoli et al. [31] of clamped–clamped Ti–6Al–4V–ZrO_2 FGM beams as shown in Fig. 3e is re-plotted under no thermal load, where $\bar{\tau}_{xz} = \tau_{xz}h^2/(fL^2)$, τ_{xz} is the transverse shear stress, f is the uniformly distributed load. We find $\bar{\sigma}_{x\theta}|_{X=0.195619}$ have the values −4.96E−05 on the outer surface greater amplitude than −1.41E−05 on the inner surface of Terfenol-D FGM shells due to rapid heating. Because without thermal load, there are no transverse shear stresses on the top and bottom surfaces in the FGM beams.

Secondly, the thermal effects of heat flux value under rapid heating are investigated. Fig. 4 shows the dominant normal displacement W along X of rapid heating on inner surface of the Terfenol-D FGM shells under the effects of rapid heat flux values $q_0 = 0$ J/(sm^2), 264 J/(sm^2), 528 J/(sm^2), 1055 J/(sm^2), 2110 J/(sm^2) and 3165 J/(sm^2), $T = 500$ K, $R_n = 1$, $\theta = 1$ radian, time $t = 1$ s, $h_3/h^* = 0.1$, $k_c c(t) = 0$. We find the higher amplitude of displacement can be obtained as in higher rapid heat flux value. Fig. 5 shows the dominant thermal normal stress $\bar{\sigma}_x$ on $Z = 0.4$ along X of Terfenol-D FGM shell under the effects of rapid heat flux values $q_0 = 0$ J/(sm^2), 264 J/(sm^2), 528 J/(sm^2), 1055 J/(sm^2), 2110 J/(sm^2) and 3165 J/(sm^2), $T = 500$ K, $R_n = 1$, $\theta = 1$ radian, time $t = 1$ s, $h_3/h^* = 0.1$, $k_c c(t) = 0$. The higher amplitude of normal stress can be obtained as in higher rapid heat flux value. There is no normal stress when there is no rapid heat flux value ($q_0 = 0$ J/(sm^2)). Almost linearly increasing with X on the $Z = 0.4$ surface, there are striking normal stress values on the two ends, $\bar{\sigma}_x = -4.18\text{E}-04$ at $X = 0$ and $\bar{\sigma}_x = -1.98\text{E}-03$ at $X = 1$, of rapid heat flux value $q_0 = 3165$ J/(sm^2) of Terfenol-D FGM shells under rapid heat flux effect.

Fig. 6 shows the time response of dominant normal displacement W at $X = 0.5$ of rapid heating on inner surface of the Terfenol-D FGM shells under the effects of control gain values $k_c c(t) = 0$ and -10^9 cases, $h_3/h^* = 0.1$, rapid heat flux value $q_0 = 2110$ J/(sm^2), $T = 500$ K, $R_n = 1$, $\theta = 1$ radian. The time step value 0.1 s is used in the GDQ vibration computation. When without velocity feedback $k_c c(t) = 0$, the amplitude of displacement W is linearly increasing value from −3.47E−05 to −2.53E+00 versus t (s) within 1 s. With velocity feedback and with suitable control gain value $k_c c(t) = -10^9$, the amplitude of displacement can be reduced to a smaller value. Fig. 7 shows the time response of dominant thermal normal stress $\bar{\sigma}_x$ at $X = 1$ on $Z = 0.4$ of rapid heating on inner surface of the Terfenol-D FGM shells under the effects of control gain values $k_c c(t) = 0$ and -10^9 cases, $h_3/h^* = 0.1$, rapid heat flux value $q_0 = 2110$ J/(sm^2), $T = 500$ K, $R_n = 1$, $\theta = 1$ radian. When without velocity feedback $k_c c(t) = 0$, the amplitude of thermal normal stress is linearly increasing value from −1.81E−08 to −1.32E−03 versus t (s) within 1 s. With velocity feedback and with suitable control gain value $k_c c(t) = -10^9$, the amplitude of thermal normal stress can also be reduced to a smaller value.

We also like to investigate the FGM effects of power law index value, environmental temperature value under rapid

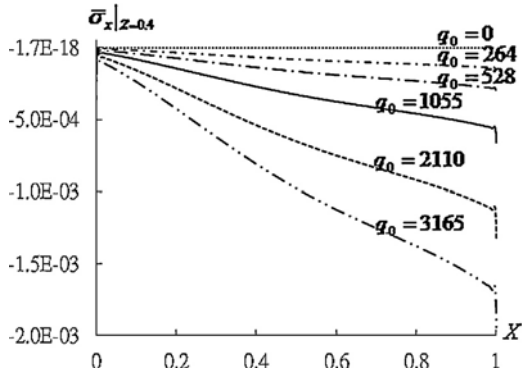

Fig. 5 – $\bar{\sigma}_x|_{Z=0.4}$ vs. X under rapid heat flux q_0.

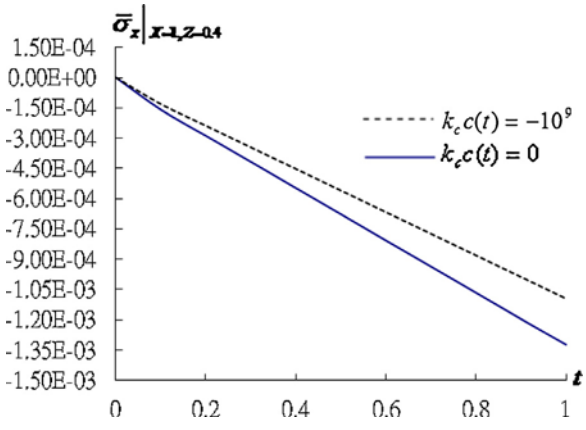

Fig. 7 – $\bar{\sigma}_x|_{X=1,Z=0.4}$ vs. t (s) of rapid heating Terfenol-D FGM shells.

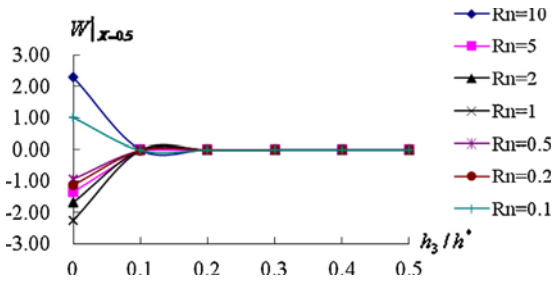

Fig. 8 – $W|_{X=0.5}$ vs. h_3/h^* under power law index R_n.

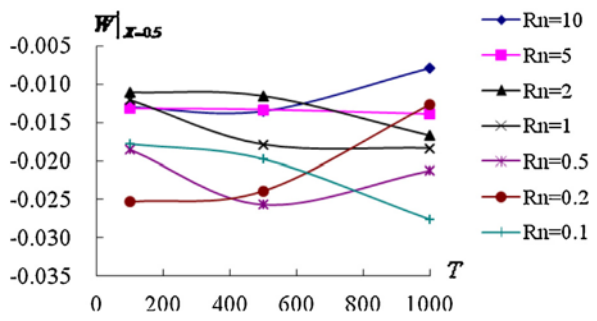

Fig. 10 – $W|_{X=0.5}$ vs. T under power law index R_n.

heating. Fig. 8 shows the dominant normal displacement W at $X = 0.5$ vs. h_3/h^* of rapid heating on inner surface of the Terfenol-D FGM shells under the effects of FGM power law index values $R_n = 0.1$, 0.2, 0.5, 1, 2, 5 and 10, $k_c c(t) = -10^9$, rapid heat flux value $q_0 = 2110\ J/(sm^2)$, $T = 500\ K$, $\theta = 1$ radian, time $t = 1$ s. We find the amplitudes of displacement decrease firstly from $h_3/h^* = 0$ to $h_3/h^* = 0.1$ then keep constant almost equal to zero from $h_3/h^* = 0.1$ to $h_3/h^* = 0.5$ for the values of $R_n = 0.1$ and 10. For the other values of R_n, the amplitudes of displacement decrease negative firstly from $h_3/h^* = 0$ to $h_3/h^* = 0.1$ then keep constant almost equal to zero. The Terfenol-D FGM shell is stable versus h_3/h^* for all values of R_n with suitable control gain value under rapid heating. Fig. 9 shows the dominant thermal normal stress $\bar{\sigma}_x$ at $X = 1$ on $Z = 0.4$ versus h_3/h^* of rapid heating on inner surface of the Terfenol-D FGM shells under the effects of FGM power law index values $R_n = 0.1$, 0.2, 0.5, 1, 2, 5 and 10, $k_c c(t) = -10^9$, rapid heat flux value $q_0 = 2110\ J/(sm^2)$, $T = 500\ K$, $\theta = 1$ radian, time $t = 1$ s. We find the amplitudes of thermal normal stress increase negative firstly from $h_3/h^* = 0$ to $h_3/h^* = 0.1$ then keep decreasing negative from $h_3/h^* = 0.1$ to $h_3/h^* = 0.5$ for the values of $R_n = 0.1$ and 10. For the other values of R_n, the amplitudes of thermal normal stress keep decreasing negative with h_3/h^* under rapid heating.

Fig. 10 shows the dominant normal displacement W at $X = 0.5$ vs. T of rapid heating on inner surface of the Terfenol-D FGM shell under the effects of FGM power law index values $R_n = 0.1$, 0.2, 0.5, 1, 2, 5 and 10, $k_c c(t) = -10^9$, rapid heat flux value $q_0 = 2110\ J/(sm^2)$, $h_3/h^* = 0.1$, $\theta = 1$ radian, time $t = 1$ s. We find the amplitudes of displacement increase negative from $T = 100\ K$ to $T = 500\ K$ then decrease negative from $T = 500\ K$ to $T = 1000\ K$ (this is an ideal temperature, the actual maximum temperature for Terfenol-D material is 653 K) for $R_n = 0.5$ and 10, almost constant from $T = 100\ K$ to $T = 500\ K$ then increase negative from $T = 500\ K$ to $T = 1000\ K$ for $R_n = 2$, increase negative from $T = 100\ K$ to $T = 500\ K$ then almost constant from $T = 500\ K$ to $T = 1000\ K$ for $R_n = 1$, all decrease negative for $R_n = 0.2$, all increase negative for $R_n = 0.1$, all constant for $R_n = 5$. With power law index values $R_n = 0.2$ and 10, the Terfenol-D FGM shell can stand against the higher temperature of environment under rapid heating. Fig. 11 shows the dominant thermal normal stress $\bar{\sigma}_x$ at $X = 1$ on $Z = 0.4$ versus T of rapid heating on inner surface of the Terfenol-D FGM shells under the effects of FGM power law index values $R_n = 0.1$, 0.2, 0.5, 1, 2, 5 and 10, $k_c c(t) = -10^9$, rapid heat flux value $q_0 = 2110\ J/(sm^2)$, $h_3/h^* = 0.1$, $\theta = 1$ radian, time $t = 1$ s. We find the amplitudes of thermal normal stresses increase negative from $T = 100\ K$ to $T = 500\ K$ then decrease negative from $T = 500\ K$ to $T = 1000\ K$ for $R_n = 1$, 2, 5 and 10, all increase negative for $R_n = 0.1$, 0.2 and 0.5 under rapid heating.

The effect of the rapid heating q_0 values on frequency parameter f^* values for different mode numbers n are investigated with different power index R_n for FGM material. The f^* values vs. n of Fig. 12a–c with $R_n = 0.1$, 1 and 10 are presented for the forced vibration at displacement component $U(L/2)$, $R/h = 500$, $L/R = 10$, $T = 500\ K$, $\theta = 1$ radian, $t = 1$ s, $h_3/h^* = 0.1$, $k_c c(t) = 0$ under $q_0 = 264$, 528, 1055 and 2110 $J/(sm^2)$. The rapid heating q_0 values only have small effects on the frequency parameter f^* values for different mode numbers n at $U(L/2)$, $t = 1$ s. The compared and referred data as shown in Fig. 12d is re-plotted for the silicon nitride-nickel FGM cylindrical shell under external pressure value $k_e = 1.2531e11$, and the classical shell theory (CST) under simply supported ends in 2010 by Sepiani et al. [32]. Fig. 12 shows the similar tendency of f^* and non-dimensional fundamental frequency Ω versus n, where $\Omega = 4\pi\omega R\sqrt{I_1/A_{11}}$, I_1 is the mass inertia, but the different scalar values between two plots occur are acceptable

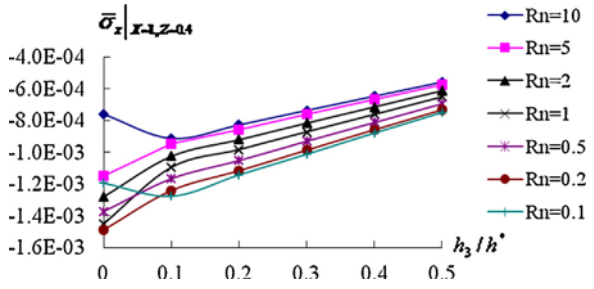

Fig. 9 – $\bar{\sigma}_x|_{X=1,Z=0.4}$ vs. h_3/h^* under power law index R_n.

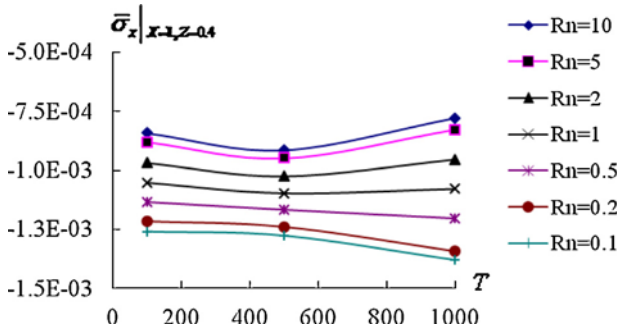

Fig. 11 – $\bar{\sigma}_x|_{X=1,Z=0.4}$ vs. T under power law index R_n.

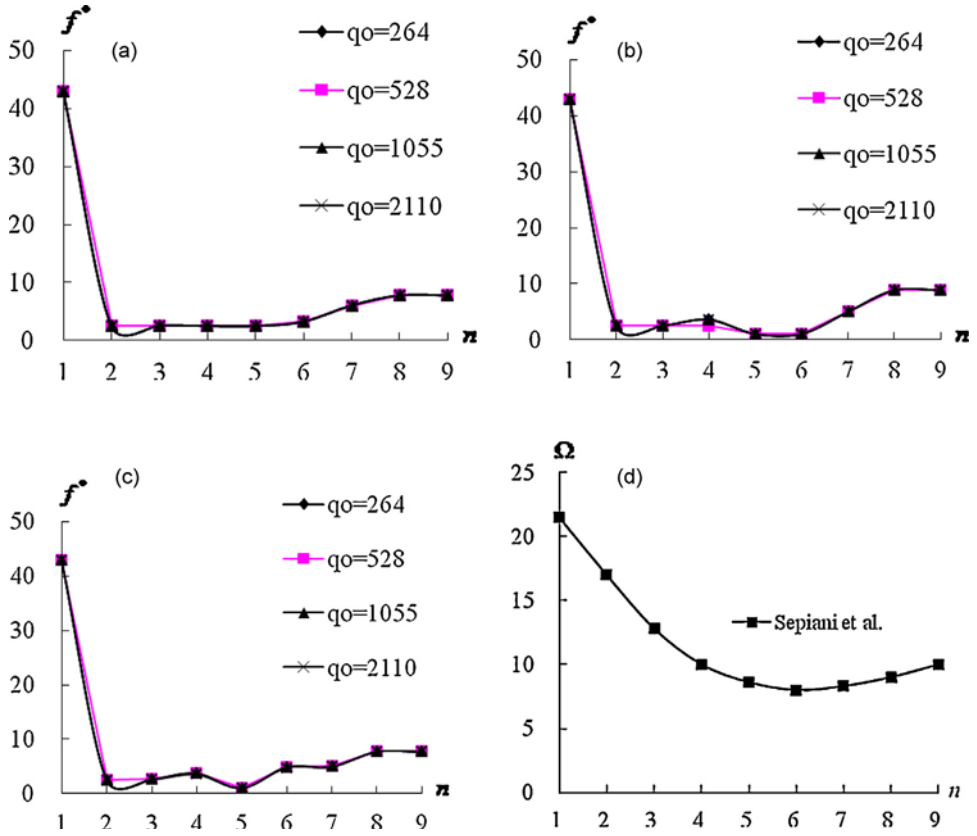

Fig. 12 – f^* vs. n of q_0 for $R_n = 0.1$, 1 and 10 and compared Ω vs. n. (a) f^* vs. n for $R_n = 0.1$. (b) f^* vs. n for $R_n = 1$. (c) f^* vs. n for $R_n = 10$. (d) compared Ω vs. n.

for the available referred data in different materials and external forced vibrations.

Finally, the transient responses of displacement and stress of rapid heating on inner surface of the Terfenol-D FGM shells under the effects of control gain values $k_c c(t) = 0$ and -10^9, $h_3/h^* = 0.1$, rapid heat flux value $q_0 = 1055$ J/(sm^2), $T = 500$ K, $R_n = 1$, $\theta = 1$ radian are investigated. The time step value 0.001 sec is used in the GDQ transient computation. Fig. 13 shows the transient value of dominant normal displacement W at $X = 0.5$ vs. t within 0.2 s. In the case of

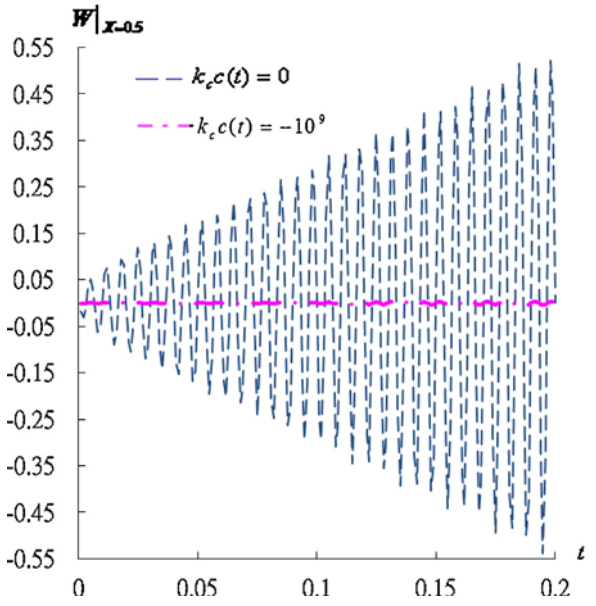

Fig. 13 – Transient $W|_{X=0.5}$ vs. t of rapid heating Terfenol-D FGM shells.

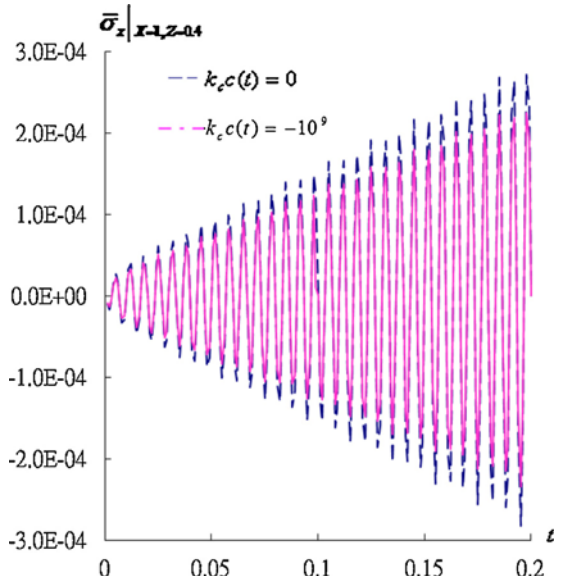

Fig. 14 – Transient $\bar{\sigma}_x|_{X=1,Z=0.4}$ vs. t of rapid heating Terfenol-D FGM shells.

control gain values $k_c c(t) = 0$, the amplitude of displacement diverges with time. In the case of velocity feedback with suitable control gain value $k_c c(t) = -10^9$, the amplitude of displacement can be reduced to a very smaller value near 0.000 under rapid heating. Fig. 14 shows the transient value of dominant thermal normal stress $\bar{\sigma}_x$ at $X = 1$ on $Z = 0.4$ vs. t within 0.2 s. We find the amplitude of stress diverges with time in the two cases of control gain values $k_c c(t) = 0$ and -10^9. In the case of velocity feedback with suitable control gain value $k_c c(t) = -10^9$ can reduce the amplitude of normal stress to a smaller value under rapid heating.

4. Conclusions

The GDQ method can be applied to calculate the numerical results of displacement and thermal stresses without the effects of shear deformation in the magnetostrictive FGM shell subjected to thermal vibration and transient response of rapid heating on inner surface of the circular cylindrical shells. By using the velocity feedback control and with suitable product of coil constant and control gain value can reduce the amplitudes of displacement and thermal stresses to a smaller value. The displacement of Terfenol-D FGM circular cylindrical shell is stable versus the Terfenol-D thickness for all power law index values of FGMs. The Terfenol-D FGM shell can stand against the higher temperature of environment with some power law index values under rapid heating. The similar tendency of frequency parameter f^* and Ω versus mode shape n, but the different scalar values occur between two plots are acceptable for the available referred data in different materials and external forced vibrations.

REFERENCES

[1] St. Kugler, P.A. Fotiu, J. Murin, The numerical analysis of FGM shells with enhanced finite elements, Engineering Structures 49 (2013) 920–935.

[2] H.R. Mollarazi, M. Foroutan, R. Moradi-Dastjerdi, Analysis of free vibration of functionally graded material (FGM) cylinders by a meshless method, Journal of Composite Materials 46 (2012) 507–515.

[3] I.A. Guz, Y.A. Zhuk, C.M. Sands, Analysis of the vibrationally induced dissipative heating of thin-wall structures containing piezoactive layers, International Journal of Non-Linear Mechanics 47 (2012) 105–116.

[4] A. Alibeigloo, A.M. Kani, M.H. Pashaei, Elasticity solution for the free vibration analysis of functionally graded cylindrical shell bonded to thin piezoelectric layers, International Journal of Pressure Vessels and Piping 89 (2012) 98–111.

[5] C.S. Chen, C.Y. Lin, R.D. Chien, Thermally induced buckling of functionally graded hybrid composite plates, International Journal of Mechanical Sciences 53 (2011) 51–58.

[6] Y. Ootao, M. Ishihara, K. Noda, Transient thermal stress analysis of a functionally graded magneto-electro-thermoelastic strip due to nonuniform surface heating, Theoretical and Applied Fracture Mechanics 55 (2011) 206–212.

[7] O. Civalek, Linear vibration analysis of isotropic conical shells by discrete singular convolution (DSC), Structural Engineering and Mechanics 25 (2007) 127–130.

[8] O. Civalek, A parametric study of the free vibration analysis of rotating laminated cylindrical shells using the method of discrete singular convolution, Thin-Walled Structures 45 (2007) 692–698.

[9] O. Civalek, Free vibration analysis of composite conical shells using the discrete singular convolution algorithm, Steel and Composite Structures 6 (2006) 353–366.

[10] R.K. Bhangale, N. Ganesan, C. Padmanabhan, Linear thermoelastic buckling and free vibration behavior of functionally graded truncated conical shells, Journal of Sound and Vibration 292 (2006) 341–371.

[11] E. Manoach, P. Ribeiro, Coupled, thermoelastic, large amplitude vibrations of Timoshenko beams, International Journal of Mechanical Sciences 46 (2004) 1589–1606.

[12] H. Cho, G.A. Kardomateas, Thermal shock stresses due to heat convection at a bounding surface in a thick orthotropic cylindrical shell, International Journal of Solids and Structures 38 (2001) 2769–2788.

[13] S. Wojciechowski, New trends in the development of mechanical engineering materials, Journal of Materials Processing Technology 106 (2000) 230–235.

[14] J.S. Chang, J.W. Shyong, Thermally induced vibration of laminated circular cylindrical shell panels, Composites Science and Technology 51 (1994) 419–427.

[15] N.N. Huang, T.R. Tauchert, Large-amplitude vibration of graphite-reinforced aluminum cylindrical panels subjected to rapid heating, Computer Engineering 3 (1993) 557–566.

[16] G.D. Manolis, D.E. Beskos, Thermally induced vibrations of beam structures, Computer Methods in Applied Mechanics and Engineering 21 (1980) 337–355.

[17] K. Shirakawa, Dynamic response of an orthotropic cylindrical shell to rapid heating, Journal of Sound and Vibration 83 (1982) 27–35.

[18] C.C. Hong, Transient response of magnetostrictive functionally graded material square plates under rapid heating, Journal of Mechanics 29 (2013) 135–142.

[19] C.C. Hong, Rapid heating induced vibration of magnetostrictive functionally graded material plates, Transactions of the ASME, Journal of Vibration and Acoustics 134 (2012), 021019-1–021019-11.

[20] C.C. Hong, Transient responses of magnetostrictive plates by using the GDQ method, European Journal of Mechanics – A: Solids 29 (2010) 1015–1021.

[21] C.C. Hong, Computational approach of piezoelectric shells by the GDQ method, Composite Structures 92 (2010) 811–816.

[22] C.C. Hong, Rapid heating induced vibration of a laminated shell with the GDQ method, The Open Mechanics Journal 3 (2009) 1–5.

[23] S.H. Chi, Y.L. Chung, Mechanical behavior of functionally graded material plates under transverse load. Part I: Analysis, International Journal of Solids and Structures 43 (2006) 3657–3674.

[24] S.J. Lee, J.N. Reddy, F. Rostam-Abadi, Nonlinear finite element analysis of laminated composite shells with actuating layers, Finite Elements in Analysis and Design 43 (2006) 1–21.

[25] S.J. Lee, J.N. Reddy, F. Rostam-Abadi, Transient analysis of laminated composite plates with embedded smart-material layers, Finite Elements in Analysis and Design 40 (2004) 463–483.

[26] H.S. Shen, Nonlinear thermal bending response of FGM plates due to heat condition, Composites Part B: Engineering 38 (2007) 201–215.

[27] C. Shu, H. Du, Implementation of clamped and simply supported boundary conditions in the GDQ free vibration analyses of beams and plates, International Journal of Solids and Structures 34 (1997) 819–835.

[28] L. Hua, K.Y. Lam, Frequency characteristic of a thin rotating cylindrical shell using the generalized differential quadrature

method, International Journal of Mechanical Sciences 40 (1998) 443–459.
[29] R.B. Hetnarski, Thermal Stresses II, Elsevier Science Publishers B.V, 1987 pp. 332–336.
[30] O. Civalek, Application of differential quadrature (DQ) and harmonic differential quadrature (HDQ) for buckling analysis of thin isotropic plates and elastic columns, Engineering Structures 26 (2004) 171–186.
[31] R. Kadoli, K. Akhtar, N. Ganesan, Static analysis of functionally graded beams using higher order shear deformation theory, Applied Mathematical Modelling 32 (2008) 2509–2525.
[32] H.A. Sepiani, A. Rastgoo, F. Ebrahimi, A. Ghorbanpour Arani, Vibration and buckling analysis of two-layered functionally graded cylindrical shell, considering the effects of transverse shear and rotary inertia, Materials and Design 31 (2010) 1063–1069.